ISSN 1682-8356
ansinet.org/ijps

INTERNATIONAL JOURNAL OF

POULTRY SCIENCE

ANSInet
308 Lasani Town, Sargodha Road, Faisalabad - Pakistan
Mob: +92 300 3008585, Fax: +92 41 8815544
E-mail: editorijps@gmail.com

International Journal of Poultry Science 5 (10): 964-969, 2006
ISSN 1682-8356

Egg Embryo Development Detection with Hyperspectral Imaging

Kurt C. Lawrence, Douglas P. Smith, William R. Windham, Gerald W. Heitschmidt and Bosoon Park
U.S. Department of Agriculture, Agricultural Research Service, P.O. Box 5677,
Russell Research Center, Athens, GA, 30604-5677, USA

Abstract: In the U. S. egg industry, anywhere from 130 million to over one billion infertile eggs are incubated each year. Some of these infertile eggs explode in the hatching cabinet and can potentially spread molds or bacteria to all the eggs in the cabinet. A method to detect the embryo development of incubated eggs was developed. Twelve brown-shell hatching eggs from two replicates (n=24) were incubated and imaged to identify embryo development. A hyperspectral imaging system was used to collect transmission images from 420 to 840 nm of brown-shell eggs positioned with the air cell vertical and normal to the camera lens. Raw transmission images from about 400 to 900 nm were collected for every egg on days 0, 1, 2, and 3 of incubation. A total of 96 images were collected and eggs were broken out on day 6 to determine fertility. After breakout, all eggs were found to be fertile. Therefore, this paper presents results for egg embryo development, not fertility. The original hyperspectral data and spectral means for each egg were both used to create embryo development models. With the hyperspectral data range reduced to about 500 to 700 nm, a minimum noise fraction transformation and a Mahalanobis Distance classification model were used to predict development. All eggs on days 2 and 3 were correctly classified (100%), while eggs from day 0 and day 1 were classified at 95.8% and 91.7%, respectively. Alternatively, the mean spectra from each egg were used to develop a partial least squares regression (PLSR) model. First, a PLSR model was developed with all eggs and all days. The data were multiplicative scatter corrected, spectrally smoothed, and the wavelength range was reduced to 539 - 770 nm. With a one-out cross validation, all eggs for all days were correctly classified (100%). Second, a PLSR model was developed with data from day 0 and day 3, and the model was validated with data from day 1 and 2. For day 1, 22 of 24 eggs were correctly classified (91.7%) and for day 2, all eggs were correctly classified (100%). Although the results are based on relatively small sample sizes, they are encouraging. However, larger sample sizes, from multiple flocks, will be needed to fully validate and verify these models. Additionally, future experiments must also include non-fertile eggs so the fertile / non-fertile effect can be determined.

Key words: Eggs, fertility, hyperspectral imaging, imaging spectroscopy, spectroscopy

Introduction

In 2005, the U. S. egg industry produced 13.1 billion hatching eggs, of which 12.4 billion were broiler eggs and 748 million were layer eggs (USDA, NASS, 2006). With fertility rates ranging from 82 to 99%, there could be anywhere from about 130 million to well over a billion infertile eggs incubated each year. These infertile eggs pose problems for the poultry industry because they take up space, reduce overall yields, have the potential to harbor bacteria or molds, and sometimes explode if left in the hatching cabinet. These "exploders" can cross-contaminate an entire hatching cabinet. In the U.S., the current practice is to candle about 5% of the eggs after ten days of incubation to estimate the fertility of the flock. Any egg that shows no development, also known as a "clear", is removed. However, there is no attempt to remove the infertile eggs from the 95% of eggs that were not candled. Clear eggs can be divided into truly infertile (more than 50% of clears), fertile but not incubated, fertile but with no development (rare), or positive development which occurs when an embryo dies but some cell growth continues and accounts for about 1% of the clears (Ernst *et al*., 2004).

There have been several attempts to detect fertility with machine vision systems. Das and Evans (1992a) identified characteristic shapes of gray-scale image histograms that were used to separate fertile from infertile white-shell eggs. Later they used neural network classifiers with the histograms to correctly classify 93.9% of the eggs at day four, 93.5% at day three, and 67.6% at day two (Das and Evans, 1992b). In both studies, the white-shell eggs were back illuminated. However, a green band-pass filter was used in the first study (Das and Evans, 1992a) while no filters were used in the second study (Das and Evans, 1992b).

Bamelis *et al*. (2002) used a halogen lamp to back illuminate both white- and brown-shell eggs. Spectroscopic measurements from 200 to 900 nm were collected. Mean transmittance at 577 nm was used to detect the hemoglobin in the fertile egg while the transmittance at 610 nm was used to normalized the results and to exclude other light absorbing effects.

Results indicated that embryonic development was detected after 108 h (4.5 days) of incubation. However, they concluded that the detection of embryonic development with visible light transmittance was not directly linked to blood formation, but with the formation of sub-embryonic fluid which occurs after 72 h. Smith *et al.* (2005) used a hyperspectral imaging system to detect fertility in both white- and brown-shell eggs with a ratio of transmittance images. They identified a ratio of a transmittance image at 576 nm divided by a transmittance image at 655 nm as effective in predicting fertility. For white-shell eggs, 91% accuracy was obtained at day three, 60% at day two and 0% at day one. For brown-shell eggs, the accuracy was 83% at day three, followed by 58% at day two and 54% at day one. Both of these studies (Bamelis *et al.*, 2002; Smith *et al.*, 2005) used one of the three well-known blood absorption bands (415, 539, and 577 nm). Measurements at 577 nm were chosen over the other absorptions because eggshells absorb most all light below 500 nm and protoporphyrin, the pigment in brown-shell eggs, has absorption peaks at 539, 589, and 643 nm (Brant *et al.*, 1953). Thus, a spectral response at 577 nm is often used to detect blood. Yet in the incubation of an egg, blood does not form until about day two. Thus, to use these ratios would limit the earliest fertility detection to sometime around day two. In this research, a multivariate analysis approach was used to determine the feasibility of detecting egg fertility at or before day two with a hyperspectral imaging system. Thus, a spectral range will be used to explore the potential of detecting embryo development without limiting the results to one of the blood wavelengths.

Materials and Methods

Hatching eggs: In each of two replicate trials, 12 broiler eggs (brown shell) were obtained from the University of Georgia (Athens, Georgia, USA) research farm (n=24) about one week apart. Eggs were incubated at the Russell Research Center in an incubator at 37.5°C (99.5 F) and 85% relative humidity. The eggs were turned automatically every hour. For each trial, the same 12 eggs were removed from the incubator, imaged with the egg air cell up (on the vertical axis), and then placed back into the incubator and imaged again on subsequent days. Thus, imaging at days 0, 1, 2, and 3 after incubation resulted in 48 images per trial for a total of 96 images. At day 6, the eggs were assessed visually for embryo development.

Imaging system: A hyperspectral imaging system, similar to one reported earlier (Lawrence *et al.*, 2003) was used to collect spectral and spatial images of eggs. A transmission imaging stand was designed to enclose the light and provide flexibility in positioning both the lights and the camera system. The hyperspectral imaging camera (Institute for Technology Development, Stennis Space Center, MS) consisted of a focusing lens, a prism-grating-prism spectrograph, a high-resolution CCD camera, a computer, and associated optical hardware. The imaging camera was designed so that the target and camera remained stationary while the lens assembly moved (Mao, 2000). The spectrograph (ImSpector V10E, Specim, Oulu, Finland) was a direct-sight spectrograph with a 30-µm slit width, an effective slit length of 14.3 mm, a 1.7-cm (2/3-in.) output image size, and C-mounts for both fore-optics and camera. The nominal spectral range was 400-1000 nm with a nominal spectral resolution of 2.8 nm. Unlike the spectrograph used in earlier work (Lawrence *et al.*, 2003), the V10E did not have a single optical axis but is canted about 17 degrees off axis. This design reduced ghost images, optical errors, and simplified calibration by effectively removing smile and keystone errors.

The spectrograph was attached to a CCD camera with a threaded locking ring and aluminum adapter plate. The purpose of the two-piece aluminum adapter plate was primarily to provide rotational alignment between the output of the spectrograph and the camera detector, and to lock the components in place once aligned. One adapter plate was attached to the bottom of the camera while the other adapter plate was mounted to the base of the translation stage. Rotational alignment between the spectrograph and camera was accomplished with locking screws in angular slots milled in the adjoining faces of the adapter plates. Focal alignment between the spectrograph and the camera was obtained by adjusting the threaded lock-ring on the spectrograph. Once aligned, the entire adapter plate was tightened to prevent movement of individual components.

The camera was a 12-bit SensiCam QE Digital Camera (Cooke Corp., Auburn Hills, MI) in a 1.7-cm (2/3-in.) format with a maximum full-frame readout time of 10 fps. The 1376 x 1040 high-resolution CCD detector had a square pixel size of 6.45 µm and was thermoelectrically cooled. Fixed to the slit end of the spectrograph was a translation stage (Model 426A, Newport Corp., Irvine, CA). The stage platform was another anodized aluminum adapter, which was threaded for a C-mount focusing lens. The focusing lens was a 1.4/17-mm C-mount lens (XNP 1.4/17-0503, Schneider Optics, Hauppage, NY). The translation stage was moved with a motorized drive and controller (Model 860A, Newport Corp., Irvine, CA). Thus, the motorized drive moved the lens assembly via the translation stage so that successive lines of the egg were scanned while the egg itself remained stationary. The egg was positioned approximately 35 cm from the focusing lens. Eggs were imaged with 325 lines with 2 x 2 binning, and a relatively long exposure time of 250 ms, which resulted in a 688 x 325 x 520 hyperspectral image. For illumination, one

Table 1: Mean Mahalanobis Distance classification results for each egg for four days of incubation. Values <1.5 have no embryo development and values ≥ 1.5 have embryo development

Set	Egg	Day 0	Day 1	Day 2	Day 3
1	1	1.05	1.92	2.00	2.00
1	2	1.00	2.00	2.00	2.00
1	3	1.00	2.00	2.00	2.00
1	4	1.00	1.61	1.99	2.00
1	5	1.00	2.00	2.00	2.00
1	6	1.01	2.00	2.00	2.00
1	7	1.00	1.95	2.00	2.00
1	8	1.90	2.00	2.00	2.00
1	9	1.00	2.00	2.00	2.00
1	10	1.00	1.97	2.00	2.00
1	11	1.00	2.00	2.00	2.00
1	12	1.00	1.99	2.00	2.00
2	13	1.01	2.00	2.00	2.00
2	14	1.00	2.00	2.00	2.00
2	15	1.00	1.87	2.00	2.00
2	16	1.00	1.43	1.99	2.00
2	17	1.00	1.97	2.00	2.00
2	18	1.00	2.00	2.00	2.00
2	19	1.00	1.98	2.00	2.00
2	20	1.02	2.00	2.00	2.00
2	21	1.00	1.75	2.00	2.00
2	22	1.00	1.99	2.00	2.00
2	23	1.00	1.41	2.00	2.00
2	24	1.00	1.99	2.00	2.00
Accuracy (%)		95.8	91.7	100.0	100.0

50-watt, MR-16, 12-V DC, tungsten-halogen lamp with a 22° beam angle was positioned 10 cm below an aluminum plate. The plate was painted flat black, and had a 2.5-cm hole positioned directly above the lamp. A rubber ring gasket was mounted around the top of the hole to limit light leaking between the egg and the hole. Attempts to calibrate the system to percent transmission with standards of known optical density were unsuccessful as no transmission standards were found to sufficiently cover the full-scale transmission range. However, the hyperspectral imaging system band numbers were calibrated to wavelengths from 420 to 840 nm (Lawrence *et al.*, 2003).

Results and Discussion

Twenty-four brown-shell eggs were used in the data analysis which consisted of two 12-egg replicates collected one week apart. All 24 eggs were found to be fertile. Therefore, the results of this experiment are not a determination of fertility, but the earliest point at which embryo development can be detected. Preliminary data analysis was performed with both the spectral and spatial information contained within the hyperspectral data. The spectral data were used to model egg embryo development. However, no morphological or textural features were found that significantly improved any of the spectral models.

Embryo development was evaluated with two methods. The first method used the original hyperspectral data to develop a two-class classification models. The second method used multivariate data analysis techniques applied to the mean spectral response of each egg to predict embryo development. Fig. 1 shows the mean spectral response of each egg set for each day of incubation. The means were the average of about 49,000 pixels, and were calculated from an egg region of interest.

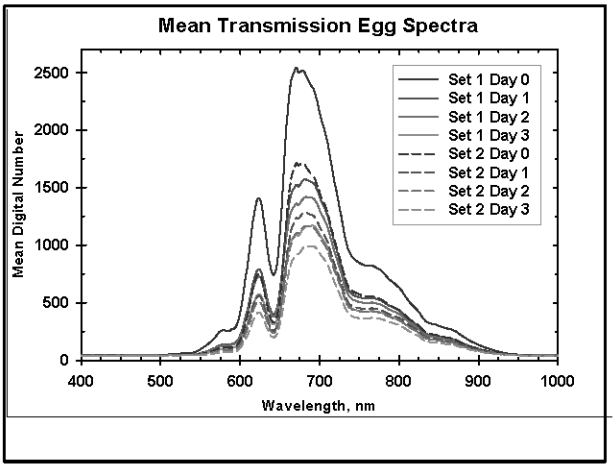

Fig. 1: Mean spectra for each day of incubation for 12 eggs for each trial.

Hyperspectral analysis: All 96 hyperspectral egg images were combined in a mosaic for simultaneous analysis with wavelength ranging from 500 to 700 nm. The background was masked with a simple threshold and erosion was performed with a 5 x 5 kernel to remove the edges from consideration. Noise from the data was removed with a minimum noise fraction (MNF) transformation (Green *et al.*, 1988) as implemented in ENVI (ITT Visual Information Solutions, Boulder, CO). A MNF transformation is essentially two cascaded principal component transformations. The first transformation uses an estimated noise covariance matrix to decorrelate and rescale the noise in the original data to unity without band-to-band correlations. Next a second principal component transformation is performed which separates the eigenvectors associated with the larger eigenvalues from the noise eigenvectors associated with the much smaller eigenvalues. These noise eigenvectors are then removed which reduces the noise and dimensionality of the data. Next a Mahalanobis Distance classification routine was used to classify the eggs into two classes, those with embryo development (fertile) or those without embryo development (no incubation). Mahalanobis Distance classification assumes that all class covariances are equal. Eggs from day 0 and day 3 were used in the classification model where no embryo development was arbitrarily assigned a value of 1 (day 0) and embryo

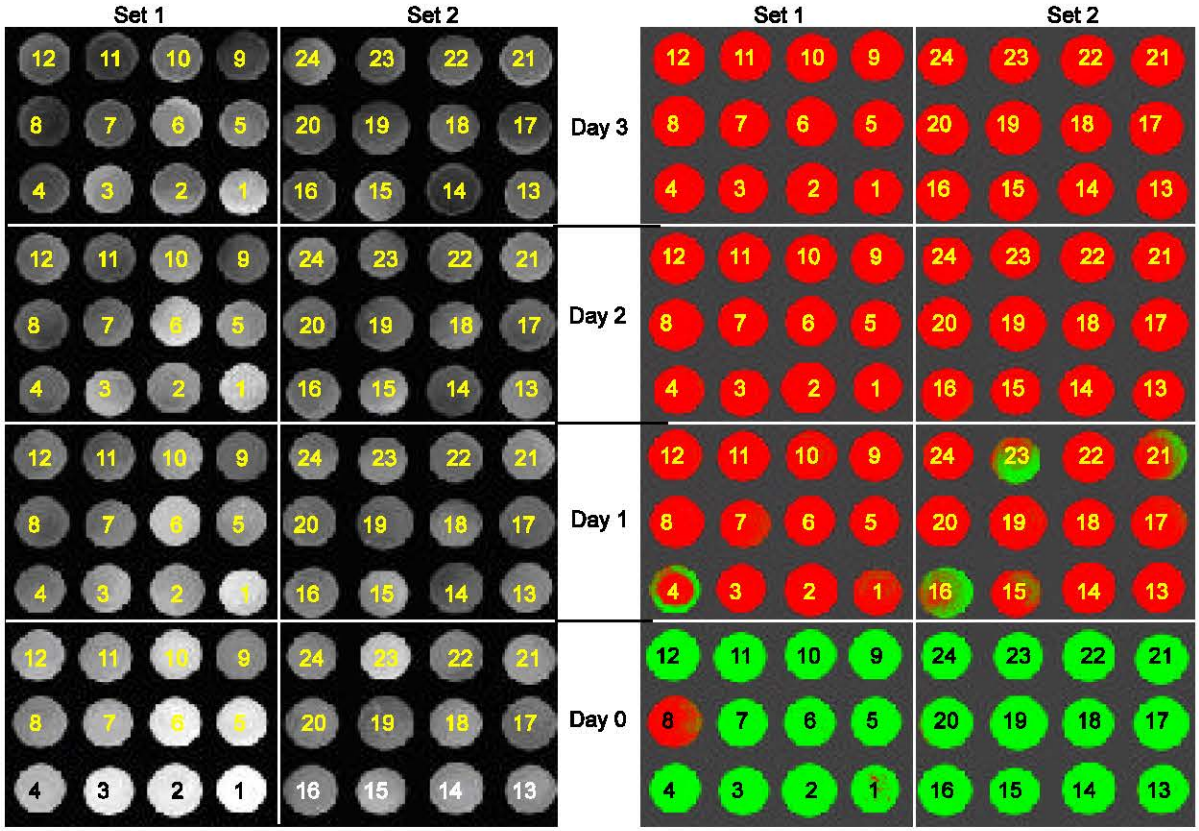

Fig. 2: Monochromatic and Mahalanobis Distance classification images of all eggs for the various days of incubation. Green (light gray in black and white) represents no embryo development (class 1) and red (dark gray in black and white) represents embryo development (class 2).

development was assigned a value of 2 (day 3). Fig. 2 shows a monochromatic mosaic of all 24 eggs during incubation and the pixel-level classification results where the color green (light gray in black/white) was assigned to no embryo development and the color red (dark gray in black/white) was assigned to pixels classified as showing embryo development. From Fig. 2, egg 8 of day 0 incorrectly appears to have embryo development while eggs 4, 15, 16, 21, and 23 of day 1 appear to have a mixed classification.

Next, using the classification results shown in Fig. 2, the mean classification values were calculated from all the pixels of each egg. Those eggs with a mean classification less than 1.5 were considered to have no embryo development. From the results shown in Table 1, egg 8 from day 0 was incorrectly classified as having embryo development while eggs 16 and 23 from day 1 were incorrectly classified as having no embryo development. Days 2 and 3 were all correctly classified. Overall 100% of day 2 and day 3 eggs were correctly classified, while day 0 and day 1 were classified at 95.8% and 91.7%, respectively.

Spectral analysis: As with the hyperspectral data, the background was removed from all images with a mask using a single threshold and an erosion filter. Regions of interest were then defined for each egg and mean spectra for each egg were calculated. Along with calibrated wavelength values, the mean spectra and arbitrary embryo development constituents (1 for no embryo development and 2 for embryo development), were output to a commercial chemometric software package for multivariate data analysis (NIRS3, Infrasoft International, Port Matilda, PA).

All days with one-out cross validation: Data were analyzed in two ways. The first method used the entire dataset to develop a partial least squares regression (PLSR) model and validate it with a standard one-out cross-validation (Martens and Naes, 1989). All data were multiplicative scatter corrected (Isaksson and Naes, 1988) to help remove some of the intensity variations associated with egg size and shell thickness, and a PLSR model was developed with the entire spectrum. Since linear regression was used instead of discriminate analysis for two-category classification, the coefficients in the regression model were proportional to canonical variate weights (Naes *et al.*, 2002). As can be

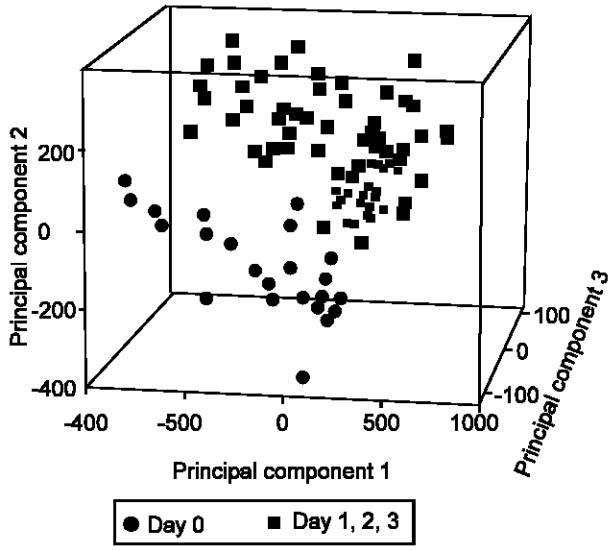

Fig. 3: Principal component score plot of all days. The plot is the projection of the original data onto principal component space for principal components 1, 2, and 3.

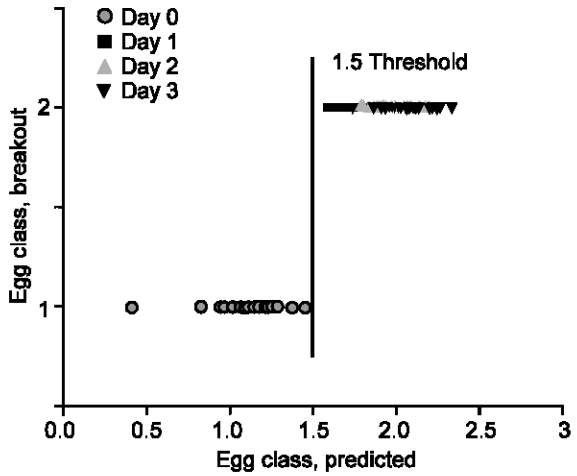

Fig. 4: Prediction results from the one-out cross validation using all eggs and all days for model development. No embryo development is designated 1 and embryo development is designated 2.

seen from Fig. 1 and confirmed by additional model development, removing transmission values below about 540 nm did not affect the model accuracy. Next, the upper wavelength range was reduced just to the point where appreciable model degradation began. Finally, wavelengths were skipped to further reduce the dataset. Results indicated that the optimum transmission measurement range was 539 to 770 nm using every 3rd data point (about 4 nm), for a total of 61 points per spectra. Fig. 3 shows a principal component

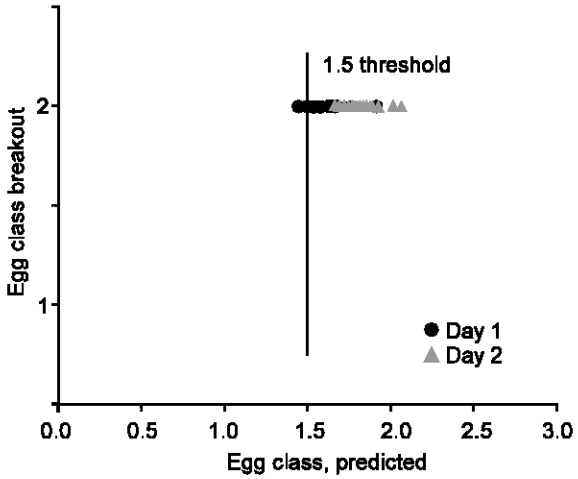

Fig. 5: Validation results for day 1 and day 2 using model developed from day 0 and day 3. No embryo development is designated 1 and embryo development is designated 2.

score plot for principal components 1, 2, and 3. A sample score is the projection of the original data onto the principal component space (eigenvector). Sample score plots are useful for determining the separation of classes based on the plotted scores. Fig. 3 shows a distinct separation between day 0 and all other days except for egg 8 from day 0, set 1. This is the same egg that the hyperspectral analysis incorrectly classified on day 0. Using the reduced wavelength range (539-770 nm) and all 96 egg mean spectra with a nine-point running average (spectral smooth), the PLSR model needed 4 terms to fit, but not over fit the data. This model accounted for 79.2% of the total variation and resulted in a standard error of cross validation (SECV) of 0.187 and a (1-variance ratio) value of 0.818. With one-out cross validation, (1-variance ratio) can be considered as the coefficient of determination. The four-term PLSR model resulted in 100% prediction accuracy for all days. Fig. 4 shows the results from the one-out cross validation where all eggs were correctly classified with the mid-point threshold of 1.5.

Day 0 and day 3 model: The second method was based on using day 0 and day 3 for model calibration and using days 1 and 2 to validate the model. The same data range (539-770nm, every 4 nm) and math treatments (nine-point running average) were used in developing the model. PLSR resulted in a five-term model with SECV = 0.154 and (1-variance ratio) = 0.91. One-out cross validation on day 0 and day 3 resulted in 100% accuracy for both days. The PLSR model was validated with day 1 and day 2 data and resulted in 91.7% (22/24) and 100% (24/24) accuracy, respectively, and the results are shown in Fig. 5. In Fig. 5, there are two eggs below

the 1.5 threshold and four eggs just above the threshold (between 1.50 and 1.55). Thus, the accuracy for day 1 might decrease if the sample population is increased.

Conclusions: A hyperspectral imaging system was successfully used to predict embryo development in 24 brown-shell eggs from day 0 to day 3 of incubation. A Mahalanobis Distance classification model using all eggs over all days resulted in an embryo classification model with 100% accuracy at day 2 and 3. Classification accuracy at day 0 and 1 were approximately 96% and 92%, respectively. Using the mean spectra for all eggs and all days as model inputs, a partial least squares regression model accurately classified all eggs for every day. Even with a model developed with 48 samples from day 0 and day 3 only, 100% classification accuracy was obtained with cross-validation for days 0 and 3. Moreover, for day 2, 100% accuracy was also obtained while for day 1, the accuracy was lower at 91.7%. The results are very encouraging. However, one must be cautiously optimistic about theses results with a limited sample population. Many more eggs from multiple flocks will be needed to fully validate and verify these models. Additionally, future experiments must also include non-fertile eggs so the fertile / non-fertile effect can be determined. Finally, since egg embryo development was identified prior to day 2, when blood formation begins, additional research is needed to identify the embryo feature(s) that the models are identifying.

References

Bamelis, F.R., K. Tona, J.G. DeBaerdemaeker and E.M. Decuypere, 2002. Detection of early embryonic development in chicken eggs using visible light transmission. Br. Poult. Sci., 43: 204-212.

Brant, A.W., K.H. Norris and G. Chin, 1953. A spectrophotometric method for detecting blood in white-shell eggs. Poult. Sci., 32: 357-363.

Das, K. and M.D. Evans, 1992a. Detecting fertility of hatching eggs using machine vision: I. histogram characterization method. Trans. ASAE, 35: 1335-1341.

Das, K. and M.D. Evans, 1992b. Detecting fertility of hatching eggs using machine vision: II. Neural network classifiers. Trans. ASAE, 35: 2035-2041.

Ernst, R.A., F.A. Bradley, U.K. Abbott and R.M. Craig, 2004. Egg candling and breakout analysis. Agric. Natural Resources, Univ. Calif. Pub., 8134: 1-9.

Green, A.A., M. Berman, P. Switzer and M.D. Craig, 1988. A transformation for ordering multispectral data in terms of image quality with implications of noise removal. IEEE Trans. Geosci. and Remote Sens., 26: 65-74.

Isaksson, T. and T. Naes, 1988. The effect of multiplicative scatter correction (MSC) and linearity improvement in NIR spectroscopy. J. Appl. Spectrosc., 42: 1273-1284.

Lawrence, K.C., B. Park, W.R. Windham and C. Mao, 2003. Calibration of a pushbroom hyperspectral imaging system for agricultural inspection. Trans. ASAE, 46: 513-521.

Mao, C., 2000. Focal plane scanner with reciprocating spatial window. U.S. Patent, 6: 166,373.

Martens, H. and T. Naes, 1989. Multivariate Calibration, Wiley, New York.

Naes, T., T. Isaksson, T. Fern and T. Davis, 2002. Multivariate Calibration and Classification. NIR Publications, Chichester, UK.

Smith, D.P., J.M. Mauldin, K.C. Lawrence, B. Park and G.W. Heitschmidt, 2005. Detection of fertility and early development of hatching eggs with hyperspectral imaging. Proc 11th European Symposium on the Quality of Eggs and Egg Products, 176-180.

USDA, NASS, 2006. Chickens and Eggs, 2005 Summary. Agric. Stat. Board, Pou., 2-4 (06).